

Susceptibility analysis of complex systems

Original

Susceptibility analysis of complex systems / Canavero, Flavio; Pignari, S.; Daniele, Vito. - STAMPA. - (1990), pp. 618-621. (Intervento presentato al convegno IEEE International Symposium on Electromagnetic Compatibility tenutosi a Washington, DC nel 21-23 Aug) [10.1109/IEMC.1990.252843].

Availability:

This version is available at: 11583/2500924 since:

Publisher:

Piscataway, N.J. : IEEE

Published

DOI:10.1109/IEMC.1990.252843

Terms of use:

This article is made available under terms and conditions as specified in the corresponding bibliographic description in the repository

Publisher copyright

(Article begins on next page)

SUSCEPTIBILITY ANALYSIS OF COMPLEX SYSTEMS

Flavio G. Canavero, Sergio Pignari and Vito Daniele

*Dipartimento di Elettronica, Politecnico,
Corso Duca degli Abruzzi 24, I-10129 Turin, Italy*

Abstract - A study of electromagnetic coupling effects on systems containing distributed elements (*e.g.*, connection wires, buses, etc.) and lumped linear components (*e.g.*, localized circuitry) is presented. The structure is decomposed into sections containing multiconductor transmission lines and interconnection blocks holding lumped elements. The external field is supposed to interfere with line sections, but mutual influences among different sections are neglected. Both the sections and the blocks are treated as multiport components and characterized by their scattering parameters. The analysis is based on a *correspondance matrix* that accounts for the topology of connections between sections and blocks. Closed-form solutions are derived in the Laplace domain, and the temporal evolution of voltages and currents at any of the system ports is obtained by a numerical inversion. This method allows us to predict the susceptibility of complex systems and to verify the intra-system compatibility (especially crosstalk). The relative influence of circuit components and of line layouts on the severity of interferences is evidenced by our simulation results.

Introduction

Electromagnetic compatibility is a highly relevant topic for the design and analysis of complex systems. In fact, the susceptibility to both external electromagnetic interferences and internal coupling effects substantially determines the performances of such systems. Lightnings, nuclear explosions, and radiated disturbances from other equipments are valid examples of external noise sources, while crosstalk and breakdowns represent cases of internally originated malfunctioning. Typical examples of networks that are particularly vulnerable are electronic and computer boards interconnected by buses, telecommunication equipment linked by cable lines, and power distribution networks.

In the past, several studies were conducted in order to assess the influence of the circuit topology on the overall system sensitivity. However, many of the existing techniques refer to computations that rely uniquely on lumped-circuit models [1]. Their approach is valid at lower frequencies, where the characteristic size of the network is negligible with respect to the interference wavelength, but the results are questionable at higher frequencies, since the wavelength can become comparable or shorter than the size of the system.

A rigorous approach to this problem must take into account the distributed nature of the transmission lines that connect different subsystems. A clear distinction must be made between networks of discrete lumped components which represent loads

or interconnection blocks, and connecting wires which must be treated as multiconductor transmission lines. Telegrapher's differential equations represent a widely accepted model for wire bundles, buses or lines of common use in electrical and electronic circuitry; additionally, any numbers of conductors are allowed by the theory [2]. Moreover, coupling with external interfering disturbances can be rigorously evaluated by means of distributed sources [3].

The analysis presented in this paper separates the system into distributed and lumped parts: each one is viewed as a multiport component and is characterized by means of its scattering parameters. This is a natural choice for the distributed element sections and it is also well suited for lumped circuits. In fact, the scattering parameters approach is compatible with the impedance or admittance matrix representation of a multiport, but it is superior in some cases: for instance, ideal line bifurcations can be specified in terms of the scattering parameters only.

The originality of this paper relies on the definition of a *correspondance matrix* that accounts for the topology of connections between sections and blocks. In fact, although the use of graph theory and scattering parameters were already proposed in the literature (see [4] and [5], respectively), our technique integrates the two approaches for the first time, and generalizes the formulation to account for interferences of both external and internal origin. The validity of the model is restricted by the limits of applicability of the telegrapher's equations and by the hypothesis of linear-element circuits.

Section two is devoted to a brief description of the method by which we are able to predict voltages and currents virtually at any accessible point of the network. Simulation results are discussed next to show the susceptibility of a system as a function of the component values and of line geometry and characteristics.

The method

The network under analysis is subdivided into transmission line sections and interconnection blocks. Each element is considered as a multiport component and is described in terms of its scattering parameters (see Fig. 1). The connecting sections are considered as multiconductor transmission lines for which the telegrapher's equations model is adopted. The interference of an external electromagnetic field is represented by distributed voltage sources proportional to the electric field component parallel to the line, and by lumped terminal sources accounting for the transverse field. The interconnection blocks are viewed as multiport networks of linear, time-invariant, passive or active lumped elements. Signal sources inside the blocks are used to

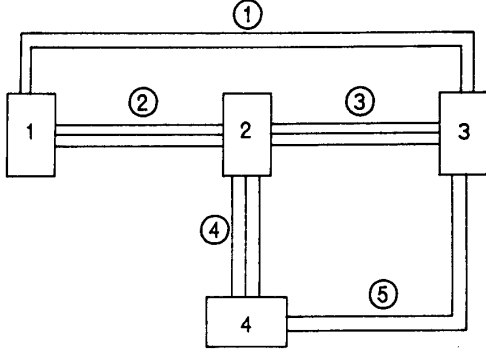


Figure 1: Block-diagram of a general complex network containing four blocks and five line sections.

study the intra-system compatibility and the internal crosstalk of the network.

In the following derivations, the voltages, currents and scattering variables of each multiport component of the system will be denoted by simply underlined vectors, while the matrices which identify impedance or scattering parameters are represented by doubly underlined symbols.

The general multiport element (*i.e.*, the n -th interconnection block or line section) is represented in terms of the scattering relationship

$$\underline{b}_x^{(n)} = \underline{S}_x^{(n)} \underline{a}_x^{(n)} + \underline{\beta}_x^{(n)}, \quad (1)$$

where the subscript x was added in order to identify lumped circuits ($x = b$) and transmission line sections ($x = s$). In this relationship, the quantities $\underline{a}_x^{(n)}$ and $\underline{b}_x^{(n)}$ represent the incident and reflected wave amplitude vectors, respectively, and are expressed in terms of the voltages $\underline{V}_x^{(n)}$ and the currents $\underline{I}_x^{(n)}$ at all ports of the network element, *i.e.*,

$$\underline{a}_x^{(n)} = \frac{1}{2} \left([\underline{Z}_{0,x}^{(n)}]^{-\frac{1}{2}} \underline{V}_x^{(n)} + [\underline{Z}_{0,x}^{(n)}]^{\frac{1}{2}} \underline{I}_x^{(n)} \right) \quad (2)$$

$$\underline{b}_x^{(n)} = \frac{1}{2} \left([\underline{Z}_{0,x}^{(n)}]^{-\frac{1}{2}} \underline{V}_x^{(n)} - [\underline{Z}_{0,x}^{(n)}]^{\frac{1}{2}} \underline{I}_x^{(n)} \right), \quad (3)$$

where $\underline{Z}_{0,x}^{(n)}$ is a diagonal matrix containing the reference impedances. The vector $\underline{\beta}_x^{(n)}$ represents the wave amplitudes flowing out of the structure, when all ports are matched to the reference impedances, and no external sources are applied. Of course, $\underline{\beta}_x^{(n)}$ depends on the sources internal to the n -th network. In particular, $\underline{\beta}_s^{(n)}$ describes the sources of internal interference which are located into localized circuitry and are responsible for the crosstalk. External electromagnetic fields are assumed to interfere with line sections only, and mutual influences among different sections are neglected. The contribution of external interferences is accounted for by distributed voltage generators along the lines and lumped voltage sources at the terminals. The effect of such sources can be translated into equivalent lumped generators located at the ends of the transmission line sections [3]. The vector $\underline{\beta}_s^{(n)}$ includes such effects. Equation (1) defines also the scattering matrix $\underline{S}_x^{(n)}$ of the network element, provided that its internal sources are switched off.

For a non-degenerate multiport, a representation in terms of the impedance matrix is possible, *i.e.*,

$$\underline{V}_x^{(n)} = \underline{Z}_x^{(n)} \underline{I}_x^{(n)} + \underline{U}_x^{(n)}, \quad (4)$$

where $\underline{Z}_x^{(n)}$ is the multiport impedance matrix and $\underline{U}_x^{(n)}$ is a voltage vector accounting for the internal sources. For such a non-degenerate multiport, the following relationships hold:

$$\underline{S}_x^{(n)} = \left([\underline{Z}_{0,x}^{(n)}]^{-\frac{1}{2}} \underline{Z}_x^{(n)} [\underline{Z}_{0,x}^{(n)}]^{-\frac{1}{2}} - \underline{1} \right) \cdot \left([\underline{Z}_{0,x}^{(n)}]^{-\frac{1}{2}} \underline{Z}_x^{(n)} [\underline{Z}_{0,x}^{(n)}]^{-\frac{1}{2}} + \underline{1} \right)^{-1} \quad (5)$$

$$\underline{\beta}_x^{(n)} = \frac{1}{2} \left(\underline{1} - \underline{S}_x^{(n)} \right) [\underline{Z}_{0,x}^{(n)}]^{-\frac{1}{2}} \underline{U}_x^{(n)}. \quad (6)$$

Complete relationships for the system under analysis can be derived if the variables characterizing each multiport circuit are grouped into arrays of larger size. In particular, voltage, current, and wave-amplitude vectors for the entire system are defined by rearranging the variables of each multiport into column vectors of dimensions $\sum_{n=1}^{N_x} M_x^{(n)}$, $M_x^{(n)}$ being the number of ports of the general n -th network, and N_x the number of networks. Thus, a generalized form of (1) is

$$\underline{b}_b = \underline{S}_b \underline{a}_b + \underline{\beta}_b, \quad (7)$$

$$\underline{b}_s = \underline{S}_s \underline{a}_s + \underline{\beta}_s, \quad (8)$$

where the complete scattering matrices \underline{S}_b and \underline{S}_s (for all the interconnection blocks and all the line sections, respectively) are block-diagonal matrices and are obtained as a composition of the matrices of the individual network elements.

The link between distributed and lumped elements is the last necessary step to solve the network equations. In fact, the wave amplitudes were so far defined at the ports of each network element, without taking into account the mutual connections. The following expressions state the equivalence of the total voltages and currents at the interfaces between line sections and interconnection blocks:

$$\underline{L}_b = -\underline{H} \underline{I}_s, \quad (9)$$

$$\underline{V}_s = \underline{H}^T \underline{V}_b. \quad (10)$$

Equation (9) defines the *correspondance matrix* $\underline{H} = [h_{ij}]$ that depends on the topology of the network and relates the section- and block- variables. In fact, the element h_{ij} takes the value of 1 if the i -th port of the ordered blocks is connected to the j -th port of the ordered line sections, and is zero otherwise. It is worth noting that, if the ports are appropriately numbered, matrix \underline{H} reduces to the identity matrix.

Simple manipulations of equations (7)-(10), with the use of (2) and (3), lead to the final expressions for the voltages and currents at the network ports:

$$\underline{V}_b = \underline{C}(\underline{A} - \underline{C})^{-1}(\underline{D} + \underline{B}) + \underline{D} \quad (11)$$

$$\underline{I}_b = (\underline{A} - \underline{C})^{-1}(\underline{D} - \underline{B}), \quad (12)$$

where the following definitions hold for the matrices \underline{A} , \underline{B} , \underline{C} , and \underline{D} :

$$\underline{A} = -(\underline{H}^T)^{-1} \underline{Z}_{0,s}^{\frac{1}{2}} (\underline{1} - \underline{S}_s)^{-1} (\underline{1} + \underline{S}_s) \underline{Z}_{0,b}^{\frac{1}{2}}, \quad (13)$$

$$\underline{B} = -2(\underline{H}^T)^{-1} \underline{Z}_{0,s}^{\frac{1}{2}} (\underline{1} - \underline{S}_s)^{-1} \underline{\beta}_s, \quad (14)$$

$$\underline{C} = \underline{Z}_{0,s}^{\frac{1}{2}} (\underline{1} - \underline{S}_s)^{-1} (\underline{1} + \underline{S}_s) \underline{Z}_{0,b}^{\frac{1}{2}}, \quad (15)$$

$$\underline{D} = 2 \underline{Z}_{0,s}^{\frac{1}{2}} (\underline{1} - \underline{S}_s)^{-1} \underline{\beta}_b. \quad (16)$$

Equations (11) and (12) quantitatively and rigorously determine the influence of a disturbance, virtually at any point of the network. Even if the previous analysis was conducted in

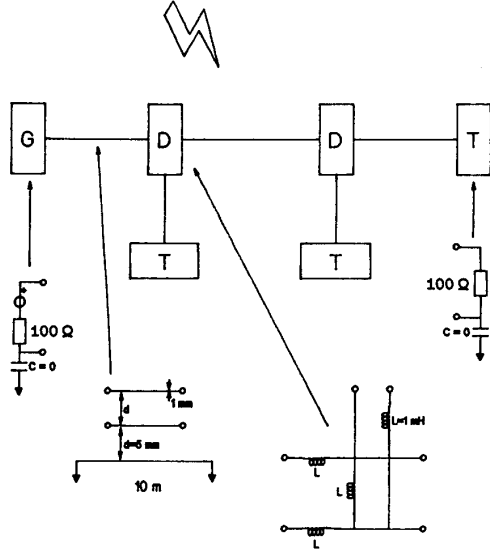


Figure 2: Example of a signal distribution network used for simulations with our method. Blocks *G* and *T* represent terminations like signal interfaces; *D* is a three-way signal splitter. The connections are realized with three-wire lines.

the Laplace variable, impulse responses are readily derived by means of an inverse transformation to the time domain. Obviously, the simplest way to perform this operation is to compute the solution of the system equations for a sufficient number of frequencies, and to use a fast Fourier transform routine for the inversion. Therefore, our results represent a powerful tool for the prediction of the overall system electromagnetic compatibility both in the frequency and in the time domain. The novelty of the approach is the application of the scattering parameters to the network elements, and the use of topological concepts to describe the connections.

Simulation results and conclusion

This section is devoted to the presentation of computer simulations of electronic subsystems linked with transmission lines. Even if the networks chosen for the analysis are very simple, they constitute good examples for evidencing the potential and the generality of our technique, and they are also representative of circuit topologies of great interest for the applications.

As a first example, we consider the structure of Fig. 2 that represents a simplified network for signal distribution. In order to study the system sensitivity to external disturbances, the transfer functions between the voltages at two ports and the incident field were computed and plotted *vs.* frequency in Fig. 3. The disturbing field is linearly polarized into the plane of the structure, and impinges with a 45°-tilt from the vertical. The diagrams of Fig. 3 show that the coupling is negligible up to 1 MHz, and that for higher frequencies there are peaks corresponding to the line resonances (*i.e.*, $f_i = c/(4\ell)$, $i = 1, 2, 3, \dots$, and ℓ being the approximate network size). The response of the network in the time domain is readily obtained by Fourier inversion of the product of the transfer function times the spectral amplitude of the interfering field. The result is shown in Fig. 4

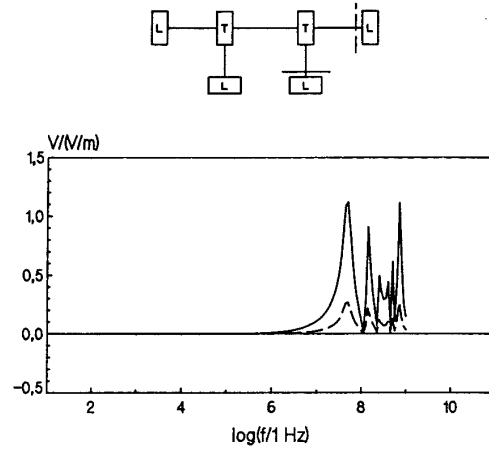


Figure 3: Transfer function between the indicated port voltages and an external interfering electric field, for the network of Fig. 2.

for an electric field $e(t) = E_0 \exp(-t/\tau)$ ($t \geq 0$, $E_0 = 50$ V/m, $\tau = 1$ μ s, and same polarization and propagation direction as above). The reflection effects due to the network terminations are evident in the diagrams of Fig. 4 as abrupt changes of the graph slope.

The vulnerability of the structure of Fig. 2 to crosstalk phenomena is presented in Fig. 5. The active internal source is placed in the leftmost block of the network (block *G*), on wire no. 1: its temporal evolution is $v(t) = V_0 \sin(\pi t/T)$, for $0 \leq t \leq T = 20$ ns, and $V_0 = 1$ V. The diagrams represent the spurious signals coupled on wire no. 2, in two load sections. Although the two load sections appear equivalent, the analysis shows that crosstalk affects one section more than the other. It follows that a rigorous simulation is important to assess the susceptibility of a system *vs.* the circuit topology and elements.

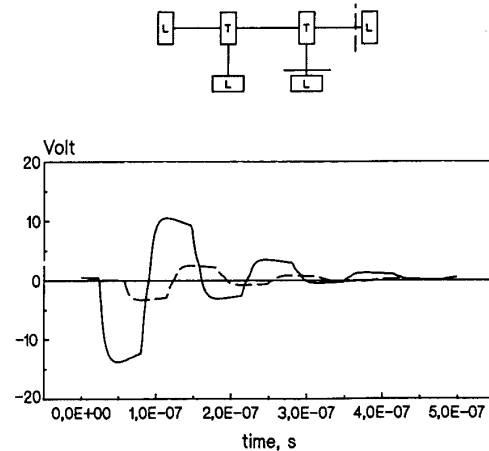


Figure 4: Time response to an external pulse for the network of Fig. 2. The diagrams represent the indicated port voltages and the interference is an exponential with a 50-V/m peak field and a time constant of 1 μ s.

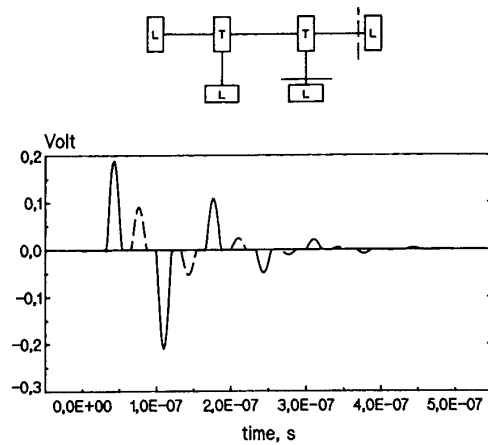


Figure 5: Example of a crosstalk simulation: time response of the network of Fig. 2 to an internal half-sine pulse with a peak amplitude of 1 V and duration of 20 ns.

A different application of our technique is presented in Fig. 6, where a simple model of a distribution network of electrical power is drawn. The network consists of a three-phase generator connected to a transformer via a three-wire line; the transformer, in turn, supplies two resistively loaded lines. The interaction with an external electromagnetic impulse simulating NEMP (50 kV/m peak voltage and $1 \mu\text{s}$ time constant) is considered. The time responses are evaluated at both ends of the line link between the transformer and a resistive load, and the result shows that the load is more protected against external interferences.

The above examples show the potential of this method to display the frequency response and the time behaviour at different places inside a complex electronic system. The network configuration may be arbitrarily complicated, and may contain distributed sections as well as lumped (passive or active) multiport components. The novelty of this technique is to employ the scattering parameters representation which is a very well suited tool for the characterization of the various parts of the network. Susceptibility analyses concerning external disturbances as well as crosstalk problems are readily performed.

Acknowledgments

This research was supported in part by the Italian Ministry of the University and Scientific Research under a grant for the *Electromagnetic Compatibility*.

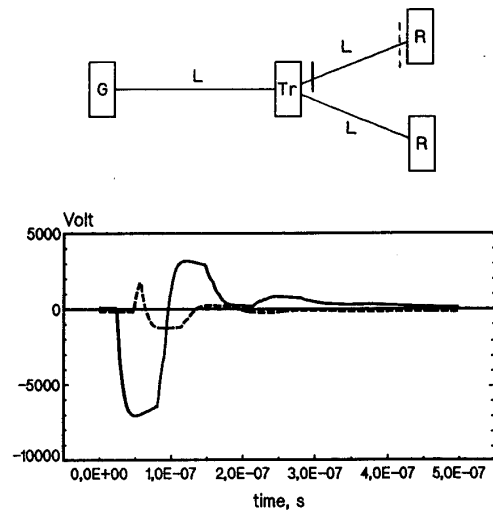


Figure 6: Time response of a power distribution network to an external NEMP impulse (50 kV/m peak field and $1 \mu\text{s}$ time constant). Block *G* is a three-phase generator, *Tr* is a transformer and *R* are resistive loads. Sections *L* are three-wire lines whose length is 100 m.

References

- [1] J. L. N. Violette, D. R. J. White, M. F. Violette: *Electromagnetic Compatibility Handbook*. Van Nostrand, New York, 1987, 707 pp.
- [2] A.R. Djordjevic, T.K. Sarkar, and R.F. Harrington, "Time-domain response of multiconductor transmission lines", *Proc. IEEE*, vol. 75, pp. 743-764, June 1987.
- [3] F. G. Canavero, V. Daniele, R. D. Graglia, "Electromagnetic pulse interaction with multiconductor transmission lines" (invited paper), *Electromagnetics, Special Issue on 'Electromagnetic Coupling to Transmission Lines'*, vol. 8, pp. 293-310, 1988.
- [4] W. Graf, *Guest Editor: Special Issue on Electromagnetic Topology of Large Systems*, *Electromagnetics*, vol. 6, no. 1, pp. 1-97, 1986.
- [5] A. Djordjevic, M. Bazdar, G. Vitosevic, T. Sarkar, R. F. Harrington: *Scattering parameters of microwave networks with multiconductor transmission lines: Software and user's manual*. Artech House, Boston, 1990, 158 pp.